IEEE Access
Multidisciplinary ⋮ Rapid Review ⋮ Open Access Journal

Received February 19, 2020, accepted March 24, 2020, date of publication April 2, 2020, date of current version May 1, 2020.

Digital Object Identifier 10.1109/ACCESS.2020.2985214

The Stability of Traffic Flow on Two Lanes Incorporating Driver's Characteristics Corresponding to Honk Effect Under V2X Environment

GUANGHAN PENG[1], DONGXUE XIA[2], AND SHUHONG YANG[2]
[1]College of Physical Science and Technology, Guangxi Normal University, Guilin 541004, China
[2]School of Computer Science and Communication Engineering, Guangxi University of Science and Technology, Liuzhou 545006, China

Corresponding authors: Guanghan Peng (pengguanghan@163.com) and Dongxue Xia (vdx821203@sina.com)

This work was supported in part by the National Natural Science Foundation of China under Grant 61963008 and Grant 61673168, in part by the Guangxi Natural Science Foundation under Grant 2018GXNSFAA281274 and Grant 2018GXNSFAA050020, and in part by the Doctor Scientific Research Startup Project Foundation of Guangxi Normal University, China, under Grant 2018BQ007.

ABSTRACT In this paper, a new lattice model is proposed by considering the driver's characteristics incorporating the timid and aggressive behaviors corresponding to honk effect under V2X environment for two-lane highway. The linear stability condition is obtained through linear stability analysis, which shows that the driver's characteristics play important influences on traffic stability under honk environment in two-lane system. The important finding implies that the timid driver's characteristics are more beneficial to increase the traffic stability than the aggressive one's characteristics under honk environment for two-lane highway via numerical simulation.

INDEX TERMS Lattice hydrodynamic model, driver's characteristics, traffic congestions.

I. INTRODUCTION

In recent years, traffic environment is becoming an important part of traffic research. In order to explore traffic problems, mathematical modeling is an effective method to study traffic phenomena. Therefore, a series of traffic models including macro models and micro models [1]–[11] have been proposed since traffic congestion is becoming more and more serious. Among them, the lattice model firstly proposed by Nagatani [10], [11] is an important model to study traffic problems. Subsequently, some extended lattice models have been proposed on single lane and two lanes by considering various traffic factors such as flux difference [12], [13], density difference [14]–[16] and other factors [17]–[33]. Also, Zeng *et al.* [34] gave a comprehensive overview about lattice models. However, the whistling phenomena often occurring under congested traffic environment in developing country have not been investigated in previous traffic models. Recently, some scholars developed a few traffic models including cellular automaton models [35], [36], car-following models and macro continuum models [37]–[41] with the consideration of the honk effect. Very recently, Peng *et al.* [42], [43] brought forward two extended lattice models with the consideration of the honk effect for single lane and two-lane highway. However, the honk effect incorporating driver's characteristics has not been investigated in crowded traffic flow on two lanes. With the development of V2X(Vehicle to X) technology, traffic environment information can be obtained by running drivers. Therefore, the honk information of the diverse driver's characteristics can be collected by applying V2X technology. Based on above idea, we proposed a new two-lane lattice model by incorporating the driver's characteristics under honk environment on two lanes. Also the theoretical analyses will be executed in the following section. Furthermore, simulation tests will be carried out to validate the rationality of our consideration.

The associate editor coordinating the review of this manuscript and approving it for publication was M. Saif Islam.

II. MODEL DEVELOPMENT

In 1999, Nagatani [28] presented an original lattice model of two-lane traffic flow with the consideration of lane changing rates as shown in Fig.1. The lane changing rate was set as $\gamma|(\rho_0)^2V'(\rho_0)|(\rho_{2,j-1}\text{-}\rho_{1,j})$ (or $\gamma|(\rho_0)^2V'(\rho_0)|(\rho_{1,j}\text{-}\rho_{2,j+1})$)

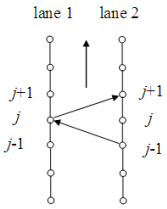

FIGURE 1. The schematic model of traffic flow on a two-lane highway.

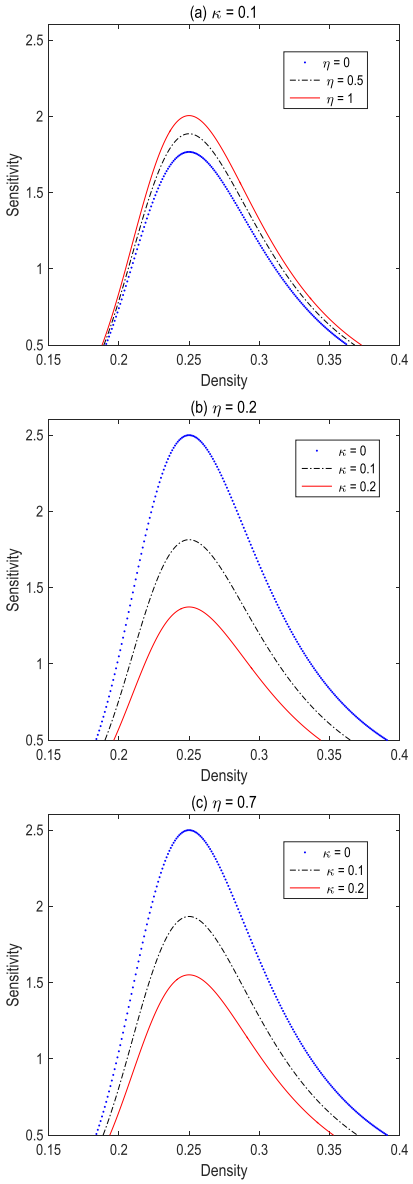

FIGURE 2. Phase diagram in parameter space (ρ; a).

from the lane 2 (or lane 1)to the lane 1 (or lane 2). Then Nagatani [28] proposed the continuity equations as follows:

$$\partial_t \rho_{1,j} + \rho_0(\rho_{1,j}v_{1,j} - \rho_{1,j-1}v_{1,j-1}) = \gamma \left|\rho_0^2 V'(\rho_0)\right| (\rho_{2,j+1} - 2\rho_{1,j} + \rho_{2,j-1}) \quad (1)$$

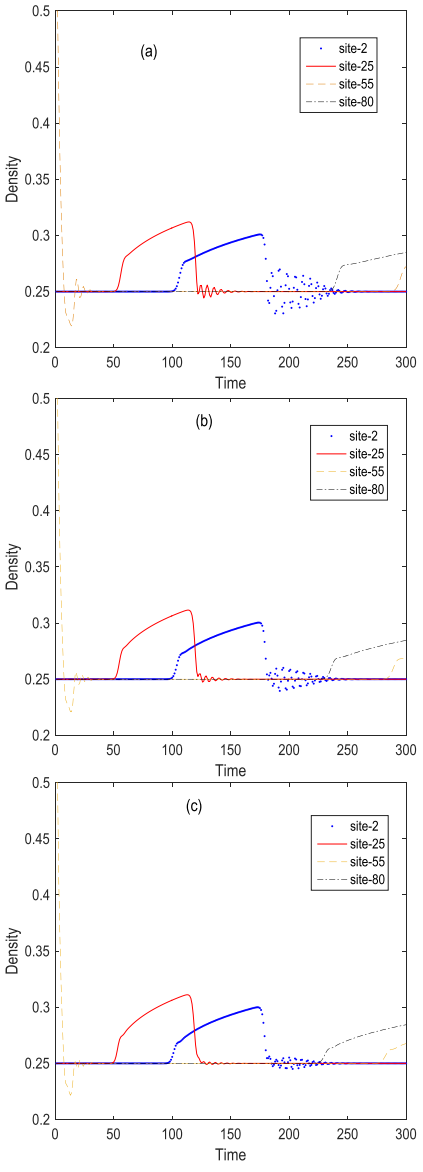

FIGURE 3. Temporal density behavior of four sites between time 1–300 s at $\kappa = 0.1$ for (a) $\eta = 1$, (b) $\eta = 0.5$, and (c) $\eta = 0$, respectively.

$$\partial_t \rho_{2,j} + \rho_0(\rho_{2,j}v_{2,j} - \rho_{2,j-1}v_{2,j-1}) = \gamma \left|\rho_0^2 V'(\rho_0)\right| (\rho_{1,j+1} - 2\rho_{2,j} + \rho_{1,j-1}) \quad (2)$$

By combining Eqs.(1) and (2), we get the following equation:

$$\partial_t \rho_j + \rho_0(\rho_j v_j - \rho_{j-1}v_{j-1}) = \gamma \left|\rho_0^2 V'(\rho_0)\right| (\rho_{j+1} - 2\rho_j + \rho_{j-1}) \quad (3)$$

where γ and ρ_0 show the rate constant coefficient with dimensionless and the average density, respectively; ρ_i and v_i respectively signify the local density and velocity. $\rho_i = (\rho_{1i} + \rho_{2i})/2$ and $\rho_i v_i = (\rho_{1i}v_{1i} + \rho_{2i}v_{2i})/2$. In addition, Nagatani [28] proposed the evolution equation as below:

$$\partial_t(q_j) = a[\rho_0 V(\rho_{j+1}) - q_j] \quad (4)$$

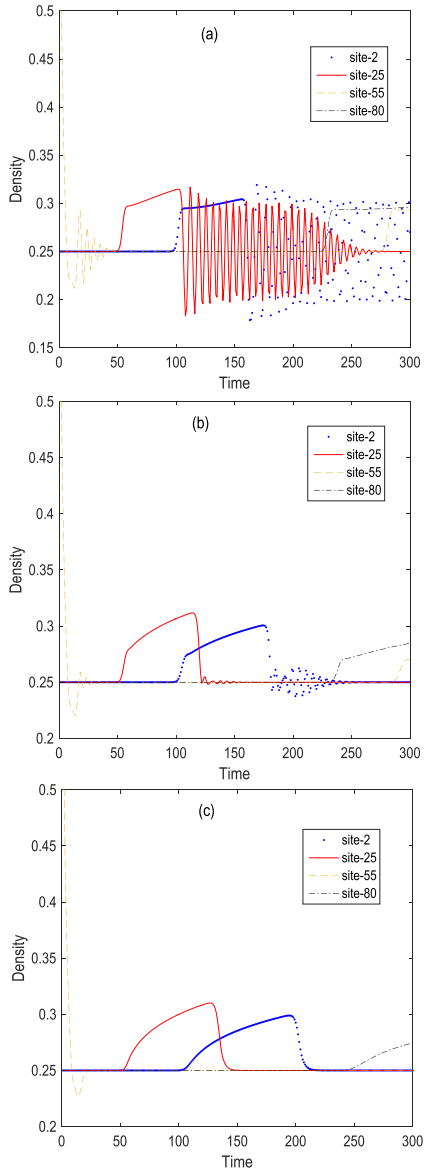

FIGURE 4. Temporal density behavior of four sites between time 1–300 s at $\eta = 0.7$ for (a) $\kappa = 0$, (b) $\kappa = 0.1$, and (c) $\kappa = 0.2$, respectively.

where $q_i = \rho_i v_i$. The sensitivity of a driver $a = 1/\tau$. The optimal velocity function $V(\rho)$ [28] was chosen as below:

$$V(\rho)=(v_{\max}/2)[\tanh(2/\rho_0 - \rho/\rho_0^2 - 1/\rho_c)+\tanh(1/\rho_c)] \tag{5}$$

Here ρ_c implies the safety density. Subsequently, Peng *et al.* [43] proposed an extended lattice model by considering the honk effect in two-lane system. But the driver's characteristics under honk environment on two lanes have not been investigated in Peng's lattice model. Consequently, we propose a new lattice model of two-lane traffic flow by incorporating the driver's characteristics corresponding to the honk effect as below:

$$\partial_t(q_j) = a[\rho_0 V(\rho_{j+1}) - q_j] + \kappa[\frac{q_m - q_j(t+\tau_1)}{\tau_1}\eta + \frac{q_m - q_j(t-\tau_2)}{\tau_2}(1-\eta)] \tag{6}$$

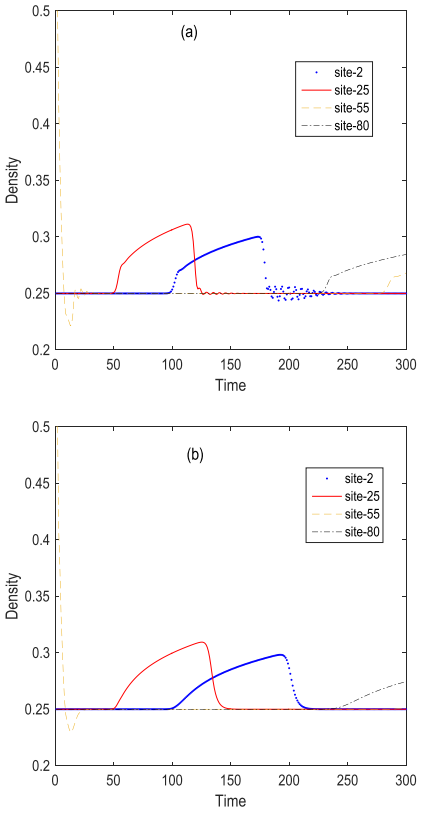

FIGURE 5. Temporal density behavior of four sites between time 1–300 s at $\eta = 0.2$ for (a) $\kappa = 0.1$ and (b) $\kappa = 0.2$, respectively.

where τ_1 and τ_2 mean the reaction time corresponding to aggressive and timid drivers under honk environment, respectively. κ shows the honk effect coefficient and η represents the proportionality coefficient for the aggressive behaviors corresponding to the honk effect. From Eq.(6), it is clear that the opposite traffic behaviors are integrated under honk environment. For simplicity, the case $\tau_1 = \tau_2 = \delta\tau$ is considered for two opposite typical behaviors corresponding to the honk effect. Henceforth, by expanding $q_j(t + \delta\tau)$ and $q_j(t\text{-}\delta\tau)$ and neglecting the nonlinear terms, we obtain: $q_j(t + \delta\tau) = q_j(t) + \delta\tau\partial_t(q_j)$ and $q_j(t\text{-}\delta\tau) = q_j(t)\text{-}\delta\tau\partial_t(q_j)$. Then Eq.(6) can be rewritten as

$$\partial_t(q_j) = a[\rho_0 V(\rho_{j+1}) - q_j] + \frac{\kappa}{\delta}\frac{q_m - q_j}{\tau} + (1-2\eta)\kappa\partial_t(q_j) \tag{7}$$

Therefore, by eliminating velocity in Eqs. (3) and (7), we obtain the differential form of the density equation as below:

$$\begin{aligned}&[1-\kappa(1-2\eta)][\rho_j(t+2\tau) - \rho_j(t+\tau)] \\ &+ \tau\rho_0^2[V(\rho_{j+1}) - V(\rho_j)] \\ &- [\frac{\kappa}{\delta} + \kappa(1-2\eta)][-\rho_j(t+\tau) + \rho_j] \\ &- [1-\kappa(1-2\eta)]\tau\gamma\left|\rho_0^2 V'(\rho_0)\right|[\rho_{j+1}(t+\tau) \\ &- 2\rho_j(t+\tau) + \rho_{j-1}(t+\tau)] - [\frac{\kappa}{\delta} + \kappa(1-2\eta)] \\ &\times \tau\gamma\left|\rho_0^2 V'(\rho_0)\right|[\rho_{j+1} - 2\rho_j + \rho_{j-1}] = 0\end{aligned} \tag{8}$$

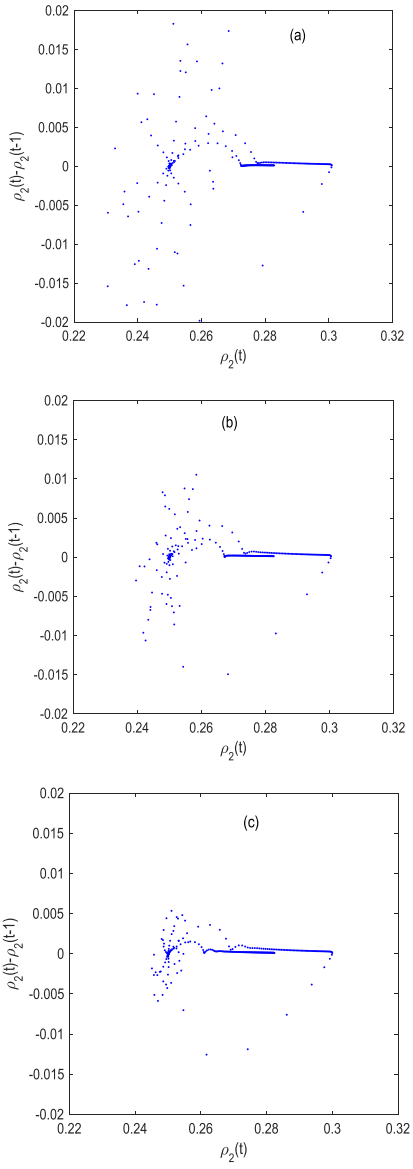

FIGURE 6. Scatter plot at site-2 between time t = 1–500 s at $\kappa = 0.1$ for (a) $\eta = 1$, (b) $\eta = 0.5$, and (c) $\eta = 0$, respectively.

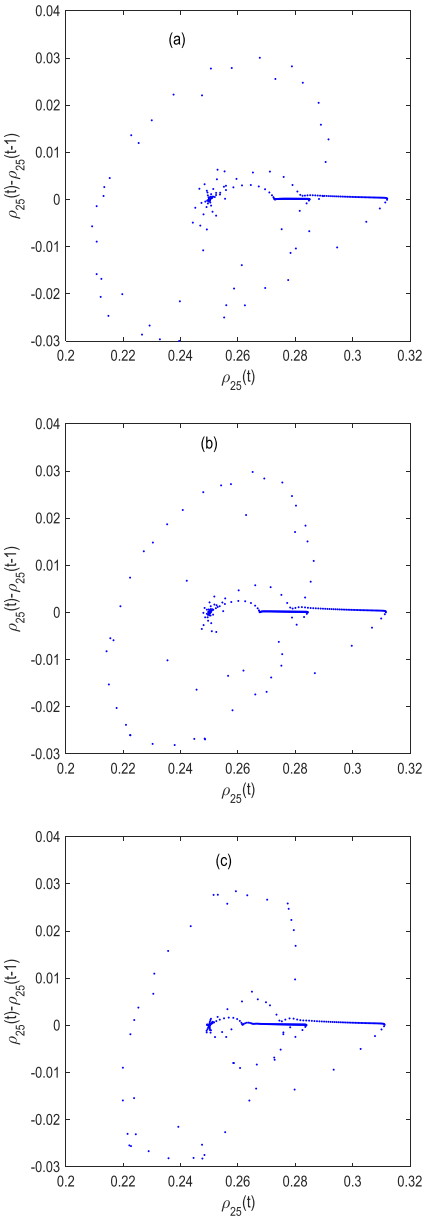

FIGURE 7. Scatter plot at site-25 between time t = 1–500 s at $\kappa = 0.1$ for (a) $\eta = 1$, (b) $\eta = 0.5$, and (c) $\eta = 0$, respectively.

III. LINEAR STABILITY ANALYSIS

The uniform traffic flow is assumed as $\rho_i(t) = \rho_0$ and $v_i = V(\rho_0)$ under the steady state. Suppose y_i be a perturbation for the local density on site j.

$$\rho_j(t) = \rho_0 + y_j(t) \tag{9}$$

By substituting Eq. (9) into Eq.(8) and linearizing it, we obtain the linearized equation as below:

$$\begin{aligned}&[1-\kappa(1-2\eta)][y_j(t+2\tau)-y_j(t+\tau)]\\&\quad+\tau\rho_0^2V'(y_{j+1}-y_j)\\&\quad-[\frac{\kappa}{\delta}+\kappa(1-2\eta)][-y_j(t+\tau)+y_j]\\&\quad-[1-\kappa(1-2\eta)]\tau\gamma\left|\rho_0^2V'(\rho_0)\right|[y_{j+1}(t+\tau)\\&\quad-2y_j(t+\tau)+y_{j-1}(t+\tau)]-[\frac{\kappa}{\delta}+\kappa(1-2\eta)]\\&\quad\times\tau\gamma\left|\rho_0^2V'(\rho_0)\right|[y_{j+1}-2y_j+y_{j-1}]=0\end{aligned} \tag{10}$$

where $V' = (\mathrm{d}V/d\rho)_{\rho=\rho 0}$. Suppose $y_i = A\exp(ikj+zt)$. Then, we acquire the equation of z as below:

$$\begin{aligned}&[1-\kappa(1-2\eta)][e^{2\tau z}-e^{\tau z}]+\tau\rho_0^2V'(e^{ik}-1)\\&\quad-[\frac{\kappa}{\delta}+\kappa(1-2\eta)][-e^{\tau z}+1]-[1-\kappa(1-2\eta)]\tau\gamma\\&\quad\times\left|\rho_0^2V'\right|[e^{ik+z\tau}-2e^{\tau z}+e^{-ik+z\tau}]-[\frac{\kappa}{\delta}+\kappa(1-2\eta)]\\&\quad\times\tau\gamma\left|\rho_0^2V'\right|[e^{ik}-2+e^{-ik}]=0\end{aligned} \tag{11}$$

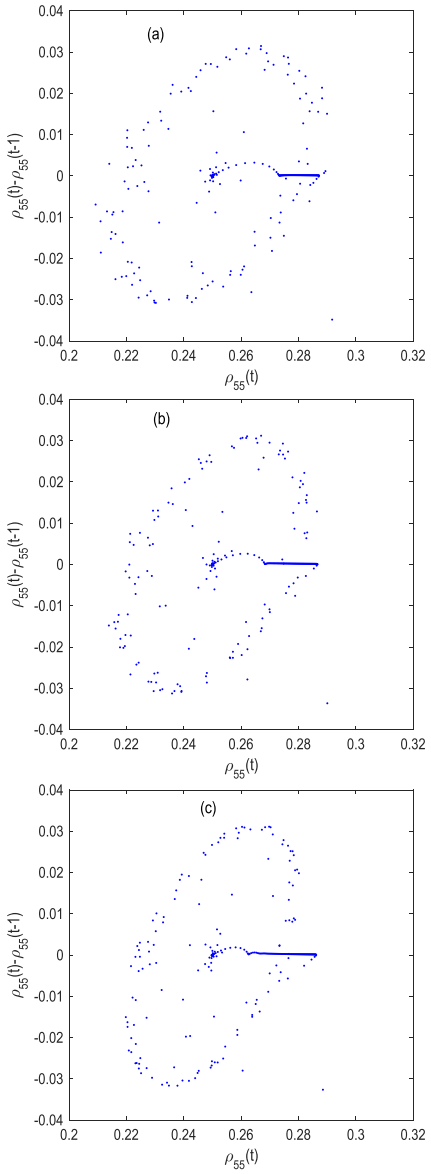

FIGURE 8. Scatter plot at site-55 between time t = 1–500 s at $\kappa = 0.1$ for (a) $\eta = 1$, (b) $\eta = 0.5$, and (c) $\eta = 0$, respectively.

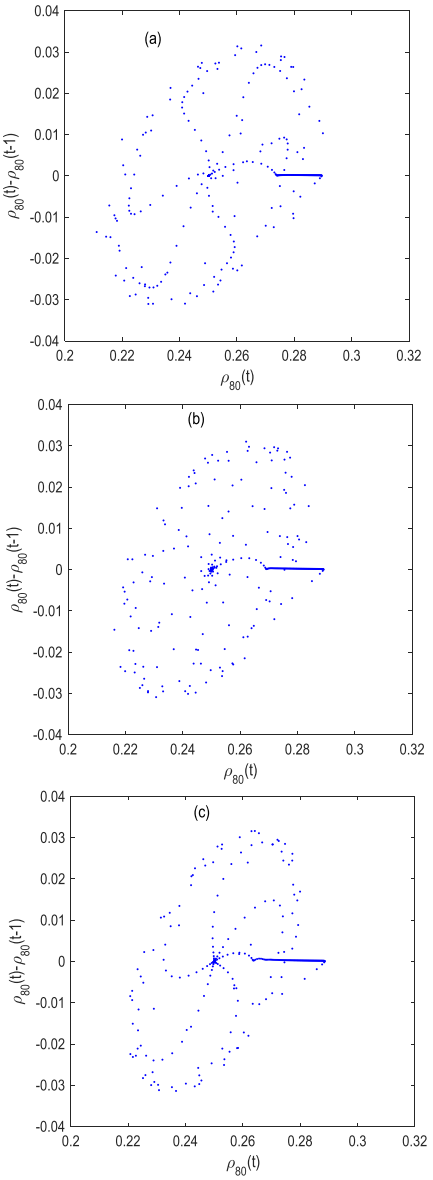

FIGURE 9. Scatter plot at site-80 between time t = 1–500 s at $\kappa = 0.1$ for (a) $\eta = 1$, (b) $\eta = 0.5$, and (c) $\eta = 0$, respectively.

In addition, we adopt the following expansion:

$$e^{2z\tau} = 1 + 2z\tau + \frac{(2z\tau)^2}{2}, e^{z\tau} = 1 + z\tau + \frac{(z\tau)^2}{2} \quad (12)$$

$$e^{ik} = 1 + ik + \frac{(ik)^2}{2}, e^{-ik} = 1 - ik + \frac{(-ik)^2}{2} \quad (13)$$

Making $z = z_1(ik)+z_2(ik)^2+\ldots$. Therefore, by ignoring the term $(ik)^n$ when $n \geq 3$, Eq.(11) can be rewritten as

$$\begin{aligned}
&[1-\kappa(1-2\eta)][\tau z_1(ik) + \tau z_2(ik)^2 \\
&+ 3\tau^2 z_1^2(ik)^2/2] + \tau\rho_0^2 V'(ik + (ik)^2/2) \\
&+ [\frac{\kappa}{\delta} + \kappa(1-2\eta)][\tau z_1(ik) + \tau z_2(ik)^2 \\
&+ \tau^2 z_1^2(ik)^2/2] + [1-\kappa(1-2\eta)] \\
&\tau\gamma\rho_0^2 V'(ik)^2 + [\frac{\kappa}{\delta} + \kappa(1-2\eta)]\tau\gamma\rho_0^2 V'(ik)^2 = 0
\end{aligned} \quad (14)$$

Thus, we get

$$\begin{aligned}
&\{[1-\kappa(1-2\eta)]z_1 + \rho_0^2 V' \\
&+ [\frac{\kappa}{\delta} + \kappa(1-2\eta)]z_1\}(ik) \\
&\{[1-\kappa(1-2\eta)]z_2 + 3[1-\kappa(1-2\eta)]\tau z_1^2/2 \\
&+ \rho_0^2 V'/2 + [\frac{\kappa}{\delta} + \kappa(1-2\eta)]z_2 \\
&+ [\frac{\kappa}{\delta} + \kappa(1-2\eta)](\tau z_1^2/2) \\
&+ (1 + \frac{\kappa}{\delta})\gamma\rho_0^2 V'\}(ik)^2 = 0
\end{aligned} \quad (15)$$

Therefore, we receive the first order and second order terms of ik as follows:

$$z_1 = \frac{-\delta\rho_o^2 V'(\rho_0)}{\delta + \kappa} \quad (16)$$

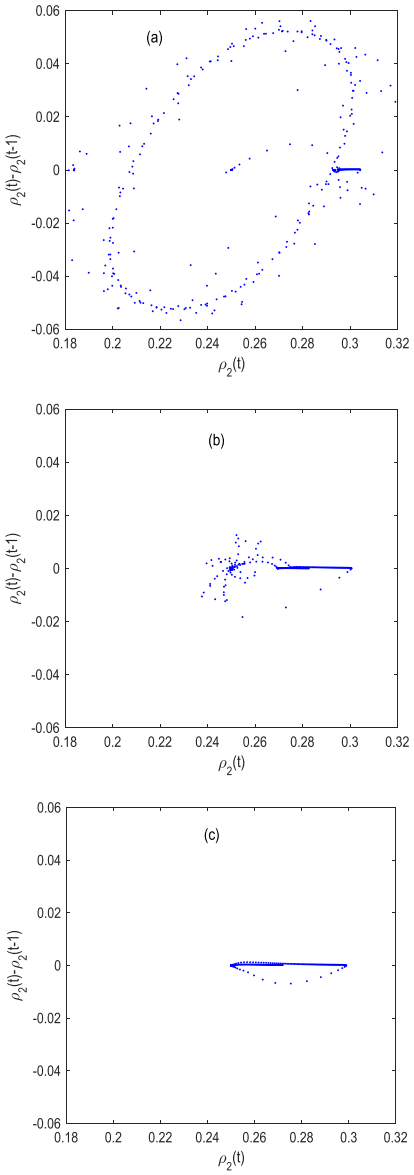

FIGURE 10. Scatter plot at site-2 between time t = 1–500 s at $\eta = 0.7$ for (a) $\kappa = 0$, (b) $\kappa = 0.1$, and (c) $\kappa = 0.2$, respectively.

$$z_2 = -\frac{[1+2(1+\kappa/\delta)\gamma]\rho_o^2 V'(\rho_0)}{2(1+\kappa/\delta)} - \frac{\tau[3+\kappa/\delta+2\kappa(2\eta-1)](\rho_0^2 V'(\rho_0))^2}{2(1+\kappa/\delta)^3} \quad (17)$$

Accordingly, the uniform steady-state flow becomes stable when $z_2 > 0$ and falls into unstable state when $z_2 < 0$. Therefore, the stable condition can be deduced by integrating the driver's characteristics under V2X environment on two lanes as below:

$$\tau < -\frac{[1+\kappa/\delta]^2 + 2\gamma[1+\kappa/\delta]^3}{[3+\kappa/\delta+2\kappa(2\eta-1)]\rho_o^2 V'(\rho_0)} \quad (18)$$

Consequently, the neutral stability condition is derived as

$$\tau = -\frac{[1+\kappa/\delta]^2 + 2\gamma[1+\kappa/\delta]^3}{[3+\kappa/\delta+2\kappa(2\eta-1)]\rho_o^2 V'(\rho_0)} \quad (19)$$

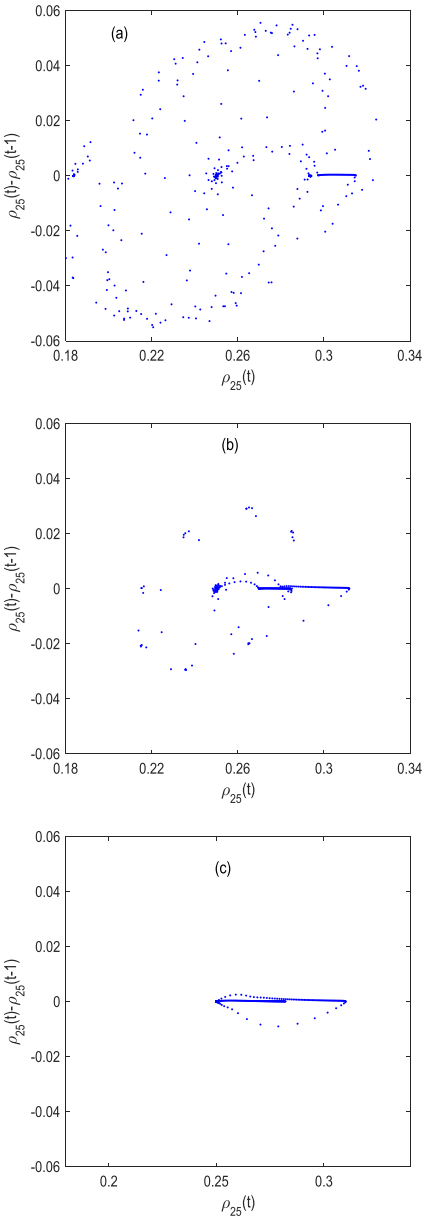

FIGURE 11. Scatter plot at site-25 between time t = 1–500 s at $\eta = 0.7$ for (a) $\kappa = 0$, (b) $\kappa = 0.1$, and (c) $\kappa = 0.2$, respectively.

Fig.2 shows the neutral stability lines under lane changing on two lanes in the space $(\rho; a)$ according to Eq.(19). Here $v_{\max} = 2$, $\delta = 0.6$ and $\gamma = 0.1$. The abscissa represents the density and the ordinate shows sensitivity in Fig. 2. From Fig.2(a), it implies that the unstable region is amplified with the increase of the proportionality η, which indicates that the more aggressive behaviors deteriorate the traffic stability and the timid behaviors improve the traffic stability with lane changing under honk environment on two lanes. In Figs. 2(b) and (c) the stable region becomes larger with the honk effect coefficient κ increasing on two lanes, which implies that the honk effect plays positive role on traffic stability for different driver' s characteristics under lane changing.

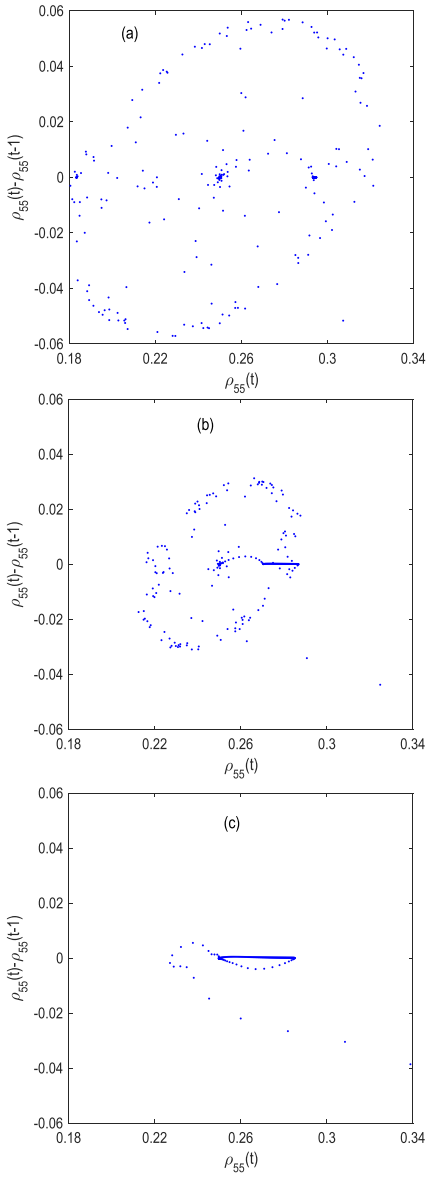

FIGURE 12. Scatter plot at site-55 between time t = 1–500 s at $\eta = 0.7$ for (a) $\kappa = 0$, (b) $\kappa = 0.1$, and (c) $\kappa = 0.2$, respectively.

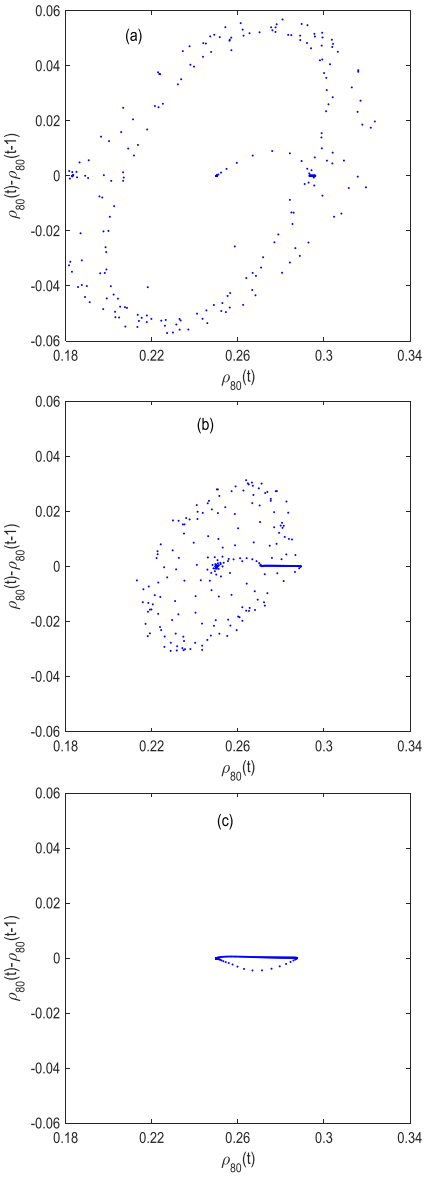

FIGURE 13. Scatter plot at site-80 between time t = 1–500 s at $\eta = 0.7$ for (a) $\kappa = 0$, (b) $\kappa = 0.1$, and (c) $\kappa = 0.2$, respectively.

IV. NUMERICAL SIMULATION

Simulation tests will be executed to investigate the influence of different driver's characteristics corresponding to the honk effect under lane changing. And the corresponding parameters are adopted as follows: $N = 140$, $a = 1.78$, $\rho_0 = 0.25$, $\gamma = 0.1$, $\delta = 0.6$ and $v_{\max} = 2$. The density of sites Nos. 50 to 55 is set as 0.5 and that of sites Nos. 56 to 60 is taken as 0.2 for initial state. Thereafter, the simulation cases for the lattices of site-2, site-25, site-55 and site-80 will be carried out for different driver's characteristics corresponding to the honk effect under lane changing.

A. EARLY TIME EFFECT WITH HONK EFFECT

Fig.3 shows the temporal density during early time 1–300 s at $\kappa = 0.1$ for $\eta = 1, 0.5$, and 0, respectively. Fig.4 means the temporal density covering early time 1–300 s at $\eta = 0.7$ for $\kappa = 0, 0.1$, and 0.2, respectively. Fig.5 represents the temporal density between time 1–300 s at $\eta = 0.2$ for $\kappa = 0.1$ and 0.2, respectively. The abscissa means the evolution time and the ordinate implies the density in Figs. 3-5. According to Fig.3, the amplitude of density becomes smaller with the proportionality coefficient η decreasing, which indicates that the timid driving behaviors contribute to traffic stability under honk environment on two lanes. In view of Figs. 4 and 5, the traffic stability is gradually enhanced as the honk coefficient κ is rising whether aggressive driving behaviors or timid driving behaviors being dominant, which implies that the honk effect always improves traffic stability.

Moreover, scatter plots are simulated as shown in Figs.6-17. The abscissa means the density $\rho_i(t)$ and the

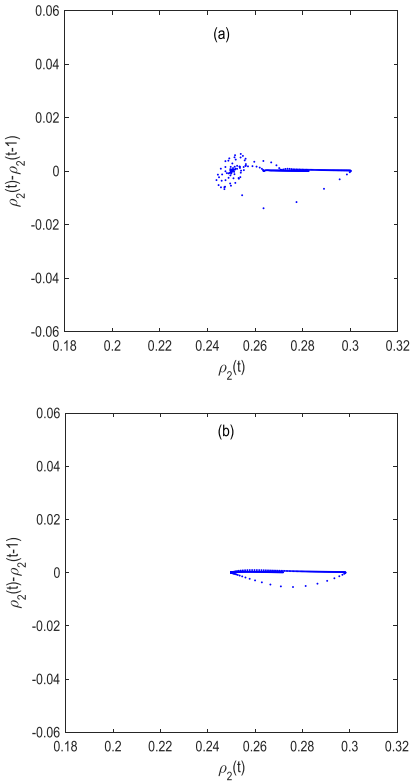

FIGURE 14. Scatter plot at site-2 between time t = 1–500 s at $\eta = 0.2$ for (a) $\kappa = 0.1$ and (b) $\kappa = 0.2$, respectively.

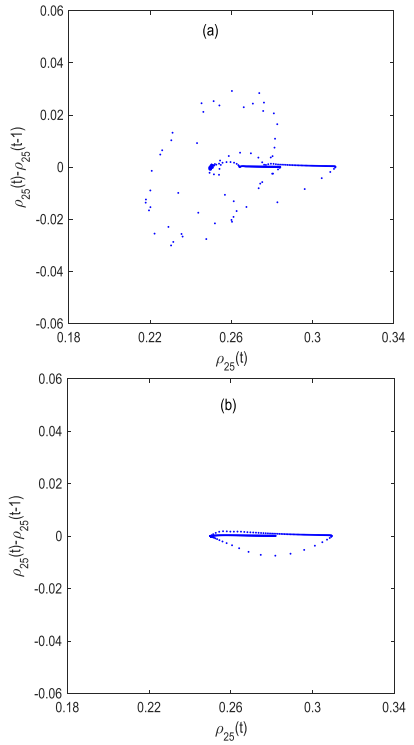

FIGURE 15. Scatter plot at site-25 between time t = 1–500 s at $\eta = 0.2$ for (a) (a) $\kappa = 0.1$ and (b) $\kappa = 0.2$, respectively.

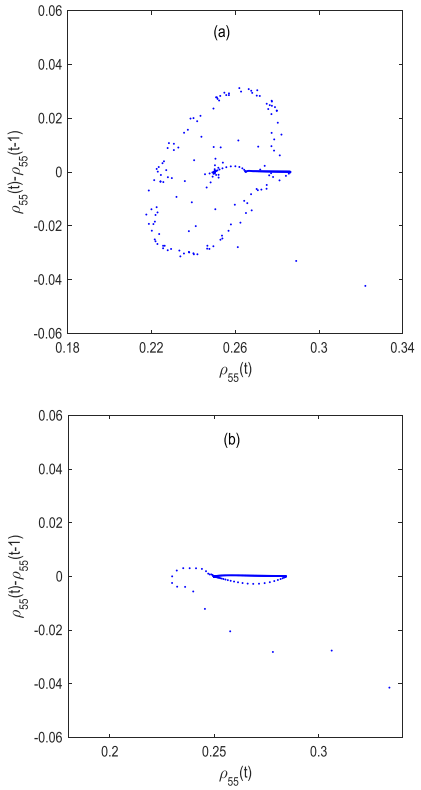

FIGURE 16. Scatter plot at site-55 between time t = 1–500 s at $\eta = 0.2$ for (a) $\kappa = 0.1$ and (b) $\kappa = 0.2$, respectively.

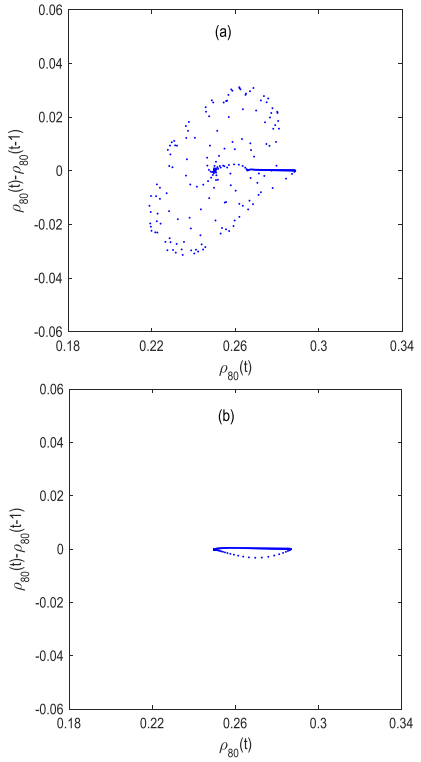

FIGURE 17. Scatter plot at site-80 between time t = 1–500 s at $\eta = 0.2$ for (a) $\kappa = 0.1$ and (b) $\kappa = 0.2$, respectively.

ordinate implies the density difference $\rho_i(t)$-$\rho_i(t$-1) at the lattices of site-2, site-25, site-55 and site-80 during time t = 1–500 s in Figs. 6-17. Figs.6-9 show the scatter plots at the lattices of site-2, site-25, site-55 and site-80 between time t = 1–500 s at κ = 0.1 for different η, respectively. From Fig. 6 to Fig. 9, scatter plots shrink with the proportionality

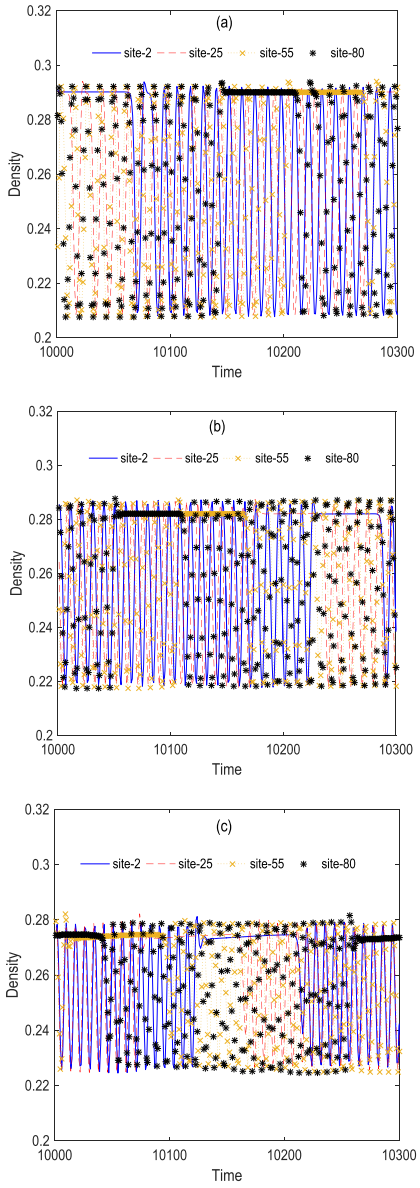

FIGURE 18. Density-time plot between time t 10,000–10,300 at $\kappa = 0.1$ for (a) $\eta = 1$, (b) $\eta = 0.5$, and (c) $\eta = 0$, respectively.

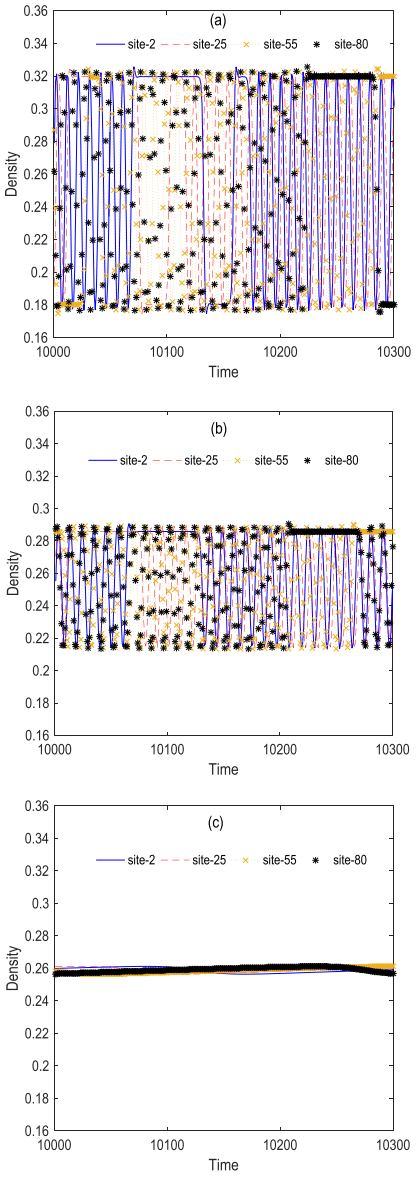

FIGURE 19. Density-time plot between time t 10,000–10,300 at $\eta = 0.7$ for (a) $\kappa = 0$, (b) $\kappa = 0.1$, and (c) $\kappa = 0.2$, respectively.

coefficient η decreasing at $\kappa = 0.1$ during time $t = 1 - 500$ s for different sites under honk environment on two lanes, which demonstrates that the timid characteristics play more positive effect on traffic flow than the aggressive characteristics under honk environment on two lanes. Figs.10-13 state the scatter plots at the lattices of site-2, site-25, site-55 and site-80 between time $t = 1 - 500$ s at $\eta = 0.7$ for different κ, respectively. Figs.14-17 represent the scatter plots at the lattices of site-2, site-25, site-55 and site-80 between time $t = 1 - 500$ s at $\eta = 0.2$ for different κ, respectively. In view of Figs.10-17, the region of scatter plots is narrowing with the increase of the honk coefficient κ for both aggressive and timid drivers. However, by comparing the aggressive behaviors and timid behaviors from Fig.10 to 17, the more timid drivers are, the more concentrated the scatter plot is. That is to say, the timid drivers contribute to traffic stability.

B. LONG-TIME (STEADY-STATE) EFFECT

Fig. 18 represents the density waves after long time 10000 s at $\kappa = 0.1$ with the different proportionality coefficient η for the lattices of site-2, site-25, site-55 and site-80 under same density initial conditions. Fig. 19 and Fig. 20 display the density waves after long time 10000 s under different honk coefficient κ for the lattices of site-2, site-25, site-55 and site-80 when $\eta = 0.7$ and 0.2 with same density initial conditions, respectively. The abscissa means time between long time 10000 -10300s and the ordinate signifies the density in Figs. 18-20. The colors in Figs. 18-20 only represent the density waves for different lattice sites. The

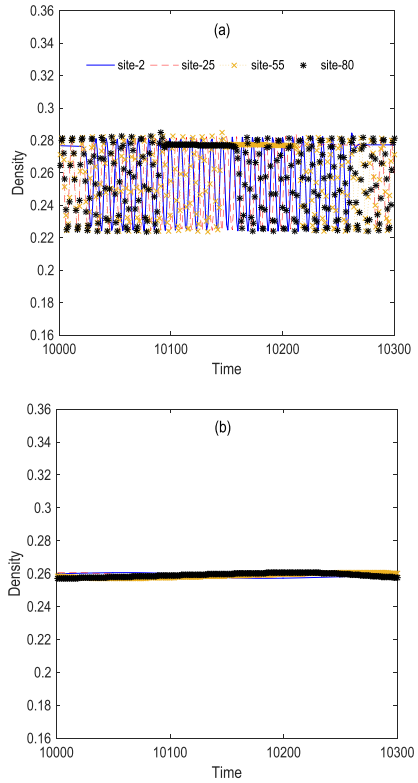

FIGURE 20. Density-time plot between time t 10,000–10,300 at $\eta = 0.2$ for (a) $\kappa = 0.1$ and (b) $\kappa = 0.2$, respectively.

smaller the amplitude of density wave is, the more stable the traffic flow is. According to Fig. 18, the amplitude of density wave decreases gradually as the proportionality coefficient η decreases under honk environment on two lanes, which implies that the timid driving behaviors are effective on traffic stability. Based on inspection of Figs. 19 and 20, the density oscillation is getting smaller and smaller as the honk coefficient κ is increasing for any driving characteristics, which indicates that honk effect can contribute to the stability of traffic flow for different driving characteristics. Obviously, the density oscillation at low value of η shrinks more rapidly than that at big value of η under same situation, which shows that appropriate timid behaviors contribute to the stability of traffic flow under honk environment on two lanes.

V. CONCLUSION SOME

Traffic environment is complex system to modeling it. This paper mainly investigated the stability of traffic flow on two lanes incorporating driver's characteristics corresponding to honk effect under V2X environment. The stability condition is closely related to the honk effect. The results show that the timid characteristics have advantages in improving traffic stability than the aggressive characteristics under honk environment on two lanes. Of course, How to make drivers timid is an interesting future work. And how to calibrate the model parameters according to the measured traffic data is our interesting research direction in the future.

REFERENCES

[1] G. F. Newell, "A simplified car-following theory: A lower order model," *Transp. Res. B, Methodol.*, vol. 36, no. 3, pp. 195–205, Mar. 2002.
[2] M. Bando, K. Hasebe, A. Nakayama, A. Shibata, and Y. Sugiyama, "Dynamical model of traffic congestion and numerical simulation," *Phys. Rev. E, Stat. Phys. Plasmas Fluids Relat. Interdiscip. Top.*, vol. 51, no. 2, pp. 1035–1042, Feb. 1995.
[3] Z. Li, W. Li, S. Xu, and Y. Qian, "Analyses of vehicle's self-stabilizing effect in an extended optimal velocity model by utilizing historical velocity in an environment of intelligent transportation system," *Nonlinear Dyn.*, vol. 80, nos. 1–2, pp. 529–540, Apr. 2015.
[4] W.-X. Zhu and H. M. Zhang, "Analysis of mixed traffic flow with human-driving and autonomous cars based on car-following model," *Phys. A, Stat. Mech. Appl.*, vol. 496, no. 4, pp. 274–285, Apr. 2018.
[5] Y. Li, C. Tang, K. Li, S. Peeta, X. He, and Y. Wang, "Nonlinear finite-time consensus-based connected vehicle platoon control under fixed and switching communication topologies," *Transp. Res. C, Emerg. Technol.*, vol. 93, no. 6, pp. 525–543, Aug. 2018.
[6] Y. Li, L. Zhang, H. Zheng, X. He, S. Peeta, T. Zheng, and Y. Li, "Nonlane-discipline-based car-following model for electric vehicles in transportation-cyber-physical systems," *IEEE Trans. Intell. Transp. Syst.*, vol. 19, no. 1, pp. 38–47, Jan. 2018.
[7] Y. Li, H. Yang, B. Yang, T. Zheng, and C. Zhang, "An extended continuum model incorporating the electronic throttle dynamics for traffic flow," *Nonlinear Dyn.*, vol. 93, no. 4, pp. 1923–1931, Sep. 2018.
[8] S. Yu, J. Tang, and Q. Xin, "Relative velocity difference model for the car-following theory," *Nonlinear Dyn.*, vol. 91, no. 3, pp. 1415–1428, Feb. 2018.
[9] J. Chen, Z. Peng, and Y. Fang, "Effects of car accidents on three-lane traffic flow," *Math. Problems Eng.*, vol. 2014, no. 7, Jan. 2014, Art. no. 413852.
[10] T. Nagatani, "Modified KdV equation for jamming transition in the continuum models of traffic," *Phys. A, Stat. Mech. Appl.*, vol. 261, nos. 3–4, pp. 599–607, Dec. 1998.
[11] T. Nagatani, "TDGL and MKdV equations for jamming transition in the lattice models of traffic," *Phys. A, Stat. Mech. Appl.*, vol. 264, nos. 3–4, pp. 581–592, Mar. 1999.
[12] Z. Li, X. Li, and F. Liu, "Stabilization analysis and modified KdV equation of lattice models with consideration of relative current," *Int. J. Mod. Phys. C*, vol. 19, no. 8, pp. 1163–1173, Aug. 2008.
[13] J.-F. Tian, B. Jia, X.-G. Li, and Z.-Y Gao, "Flow difference effect in the lattice hydrodynamic model," *Chin. Phys. B*, vol. 19, no. 4, Apr. 2010, Art. no. 040303.
[14] J.-F. Tian, Z.-Z. Yuan, B. Jia, M.-H. Li, and G.-J. Jiang, "The stabilization effect of the density difference in the modified lattice hydrodynamic model of traffic flow," *Phys. A, Stat. Mech. Appl.*, vol. 391, no. 19, pp. 4476–4482, Oct. 2012.
[15] T. Wang, Z. Gao, J. Zhang, and X. Zhao, "A new lattice hydrodynamic model for two-lane traffic with the consideration of density difference effect," *Nonlinear Dyn.*, vol. 75, nos. 1–2, pp. 27–34, Jan. 2014.
[16] A. K. Gupta and P. Redhu, "Analysis of a modified two-lane lattice model by considering the density difference effect," *Commun. Nonlinear Sci. Numer. Simul.*, vol. 19, no. 5, pp. 1600–1610, May 2014.
[17] T. Nagatani, "Jamming transition in traffic flow on triangular lattice," *Phys. A, Stat. Mech. Appl.*, vol. 271, nos. 1–2, pp. 200–221, Sep. 1999.
[18] T. Nagatani, "Jamming transition in a two-dimensional traffic flow model," *Phys. Rev. E, Stat. Phys. Plasmas Fluids Relat. Interdiscip. Top.*, vol. 59, no. 5, pp. 4857–4864, May 1999.
[19] T. Nagatani, "Jamming transition of high-dimensional traffic dynamics," *Phys. A, Stat. Mech. Appl.*, vol. 272, nos. 3–4, pp. 592–611, Oct. 1999.
[20] P. Redhu and A. K. Gupta, "Phase transition in a two-dimensional triangular flow with consideration of optimal current difference effect," *Nonlinear Dyn.*, vol. 78, no. 2, pp. 957–968, Oct. 2014.
[21] A. K. Gupta and P. Redhu, "Analyses of the driver's anticipation effect in a new lattice hydrodynamic traffic flow model with passing," *Nonlinear Dyn.*, vol. 76, no. 2, pp. 1001–1011, Apr. 2014.
[22] P. Redhu and A. K. Gupta, "Jamming transitions and the effect of interruption probability in a lattice traffic flow model with passing," *Phys. A, Stat. Mech. Appl.*, vol. 421, no. 3, pp. 249–260, Mar. 2015.
[23] A. K. Gupta and P. Redhu, "Jamming transition of a two-dimensional traffic dynamics with consideration of optimal current difference," *Phys. Lett. A*, vol. 377, nos. 34–36, pp. 2027–2033, Nov. 2013.
[24] P. Redhu and A. K. Gupta, "Effect of forward looking sites on a multi-phase lattice hydrodynamic model," *Phys. A, Stat. Mech. Appl.*, vol. 445, no. 11, pp. 150–160, Mar. 2016.

[25] G. Zhang, D.-H. Sun, H. Liu, and D. Chen, "Stability analysis of a new lattice hydrodynamic model by considering lattice's self-anticipative density effect," *Phys. A, Stat. Mech. Appl.*, vol. 486, no. 6, pp. 806–813, Nov. 2017.
[26] H.-X. Ge, Y. Cui, R.-J. Cheng, and K.-Q. Zhu, "The control method for the lattice hydrodynamic model," *Commun. Nonlinear Sci. Numer. Simul.*, vol. 22, nos. 1–3, pp. 903–908, May 2015.
[27] C. Tian, D. Sun, and M. Zhang, "Nonlinear analysis of lattice model with consideration of optimal current difference," *Commun. Nonlinear Sci. Numer. Simul.*, vol. 16, no. 11, pp. 4524–4529, Nov. 2011.
[28] T. Nagatani, "Jamming transitions and the modified Korteweg–de Vries equation in a two-lane traffic flow," *Phys. A, Stat. Mech. Appl.*, vol. 265, nos. 1–2, pp. 297–310, Mar. 1999.
[29] Z. Li, R. Zhang, S. Xu, and Y. Qian, "Study on the effects of driver's lane-changing aggressiveness on traffic stability from an extended two-lane lattice model," *Commun. Nonlinear Sci. Numer. Simul.*, vol. 24, nos. 1–3, pp. 52–63, Jul. 2015.
[30] G. Zhang, D.-H. Sun, W.-N. Liu, M. Zhao, and S.-L. Cheng, "Analysis of two-lane lattice hydrodynamic model with consideration of drivers' characteristics," *Phys. A, Stat. Mech. Appl.*, vol. 422, no. 3, pp. 16–24, Mar. 2015.
[31] A. K. Gupta and P. Redhu, "Analyses of driver's anticipation effect in sensing relative flux in a new lattice model for two-lane traffic system," *Phys. A, Stat. Mech. Appl.*, vol. 392, no. 22, pp. 5622–5632, Nov. 2013.
[32] S. Sharma, "Lattice hydrodynamic modeling of two-lane traffic flow with timid and aggressive driving behavior," *Phys. A, Stat. Mech. Appl.*, vol. 421, no. 3, pp. 401–411, Mar. 2015.
[33] S. Sharma, "Effect of driver's anticipation in a new two-lane lattice model with the consideration of optimal current difference," *Nonlinear Dyn.*, vol. 81, nos. 1–2, pp. 991–1003, Jul. 2015.
[34] Y. Zeng and N. Zhang, "Review and new insights of the traffic flow lattice model for road vehicle traffic flow," in *Proc. IEEE Int. Conf. Control Sci. Syst. Eng.*, Dec. 2014, pp. 100–103.
[35] L. Zheng, S. Ma, and S. Zhong, "Analysis of honk effect on the traffic flow in a cellular automaton model," *Phys. A, Stat. Mech. Appl.*, vol. 390, no. 6, pp. 1072–1084, Mar. 2011.
[36] B. Jia, R. Jiang, Q.-S. Wu, and M.-B. Hu, "Honk effect in the two-lane cellular automaton model for traffic flow," *Phys. A, Stat. Mech. Appl.*, vol. 348, no. 3, pp. 544–552, Mar. 2005.
[37] T. Q. Tang, H. J. Huang, and H. Y. Shang, "A macro model for bicycle flow and pedestrian flow with the consideration of the honk effects," *Int. J. Mod. Phys. B*, vol. 25, no. 32, pp. 4471–4479, Dec. 2011.
[38] T.-Q. Tang, C.-Y. Li, H.-J. Huang, and H.-Y. Shang, "An extended optimal velocity model with consideration of honk effect," *Commun. Theor. Phys.*, vol. 54, no. 6, pp. 1151–1155, Dec. 2010.
[39] T. Q. Tang, C. Y. Li, Y. H. Wu, and H. J. Huang, "Impact of the honk effect on the stability of traffic flow," *Phys. A, Stat. Mech. Appl.*, vol. 390, no. 20, pp. 3362–3368, Oct. 2011.
[40] H. Y. Wen, Y. Rong, C. B. Zeng, and W. W. Qi, "The effect of driver's characteristics on the stability of traffic flow under honk environment," *Nonlinear Dyn.*, vol. 84, no. 3, pp. 1517–1528, May 2016.
[41] H. Kuang, Z.-P. Xu, X.-L. Li, and S.-M. Lo, "An extended car-following model accounting for the honk effect and numerical tests," *Nonlinear Dyn.*, vol. 87, no. 1, pp. 149–157, Jan. 2017.
[42] G. Peng, H. Kuang, and L. Qing, "Feedback control method in lattice hydrodynamic model under honk environment," *Phys. A, Stat. Mech. Appl.*, vol. 509, no. 11, pp. 651–656, Nov. 2018.
[43] G. Peng, H. Kuang, H. Zhao, and L. Qing, "Nonlinear analysis of a new lattice hydrodynamic model with the consideration of honk effect on flux for two-lane highway," *Phys. A, Stat. Mech. Appl.*, vol. 515, no. 2, pp. 93–101, Feb. 2019.

GUANGHAN PENG received the Ph.D. degree from Chongqing University, in June 2009. He is currently a Professor with the College of Physical Science and Technology, Guangxi Normal University. His research interests cover traffic flow theory, intelligent transportation systems, and traffic control.

DONGXUE XIA is currently an Associate Professor with the School of Computer Science and Communication Engineering, Guangxi University of Science and Technology. Her research interests cover traffic flow theory, intelligent transportation systems, and machine learning.

SHUHONG YANG received the Ph.D. degree from Chongqing University, in June 2014. He is currently an Associate Professor with the School of Computer Science and Communication Engineering, Guangxi University of Science and Technology. His research interests cover traffic flow theory, intelligent transportation systems, and machine learning.